Temperature determination in a MW plasma torch and on a deposition target by modelling and experiment

M. Baeva[1], F. Hempel[1], R. Methling[1], T. Trautvetter[2] H. Baierl[2], D. Loffhagen[1] and R. Foest[1]

[1]*Leibniz Institute for Plasma Science and Technology, Greifswald, Germany*
[2]*Leibniz Institute of Photonic Technology, Jena, Germany*

Abstract: The temperature fields generated in the plasma source and in the region of treatment are key parameters due to the need for continuous operation and initiation of plasma-chemical reactions. The gas temperature in a microwave plasma source operated at atmospheric pressure and in the plume was determined by self-consistent modelling, emission spectroscopy and thermography.

Keywords: Microwave plasma, self-consistent modelling, emission spectroscopy.

1. Introduction

A microwave (MW) plasma torch operated at atmospheric pressure at a frequency of 2.45 GHz is currently studied for multi-component doping of silica preforms. The plasma source consists of a standard waveguide R26 and a quartz tube traversing at the position of maximum electric field of the fundamental mode TE_{10}. Argon/oxygen mixtures are employed as working gas. The plasma jet is directed towards a rotating substrate as it is shown in Fig. 1. For the generation of silica, precursors are fed through an additional tube placed outside the plasma source.

The determination of the plasma parameters in the region of plasma-precursor interaction is of primary importance for the technological application. On the one hand, the plasma parameters in the plume depend on the conditions inside the plasma source. On the other hand, the source is hardly accessible by diagnostics methods. Therefore, complementary studies by modelling and experiments are in progress and some of them are reported here.

Recently, a model of the plasma source has been developed [1] for the operation in pure argon. It describes in a self-consistent manner the plasma source employing the plasma, electromagnetic and hydrodynamic equations. Results of the modelling showed that the maximum electron density is obtained close to the tube wall where the plasma faces the incoming microwaves. As a result of the heat load on the wall, the operation can become critical. Further modelling studies are therefore needed in order to obtain proper flow conditions.

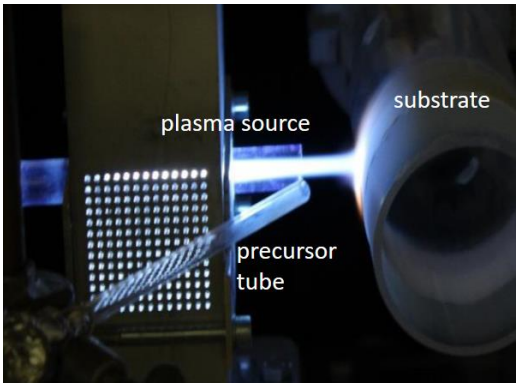

Fig. 1. Side view of the experimental setup.

The temperature fields generated in the plasma source and in the region, where the plasma jet reacts with the precursor, are key parameters due to the need for continuous operation and initiation of plasma-chemical reactions. Therefore, the computational domain has to include the plume outside the quartz tube of the plasma source so that the model predictions of gas temperature can be compared to experimental results obtained by emission spectroscopy (from the plasma zone outside the waveguide) and thermography (on the surface of the quartz tube and of the substrate).

2. Self-consistent modelling approach

A detailed description of the model is given in the recent publication [1]. Here, only the main features of the model

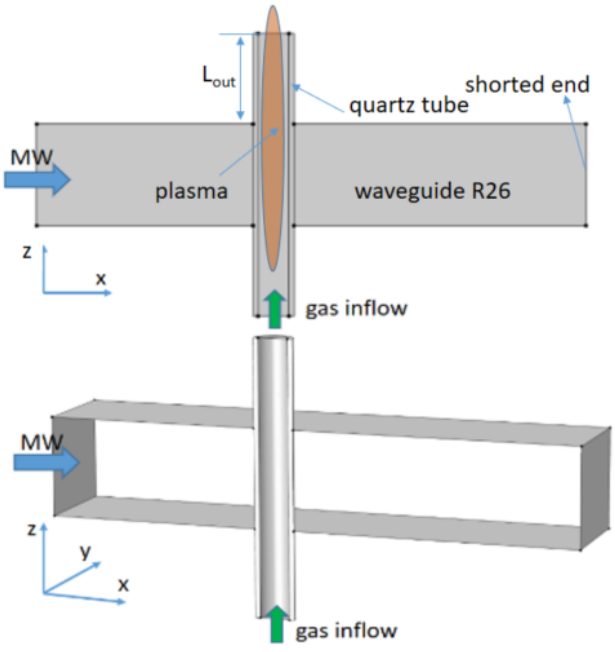

Fig. 2. Schematic view of the plasma source.

are outlined. A schematic view of the two-dimensional (2D) and three-dimensional (3D) model geometry is presented in Fig. 2. The microwave enters the waveguide, propagates along it and reflects on the short end to build a standing wave. The gas is fed into a quartz tube with an inner radius of 6.1 mm. The tube position is adjusted to match the maximum of the electric field in the waveguide to ignite the plasma. The part of the tube protruding from the resonator has the length L_{out}.

The model is based on a hydrodynamic approach. Its equations describe in a self-consistent manner the gas flow, the plasma kinetics, the heat transfer, and the microwave field in the waveguide. The Navier-Stokes equations for conservation of mass and momentum, equations for the conservation of species as well as of energy of electrons and heavy particles, and the microwave field equation are considered. The model avoids the assumption of quasi-neutrality and solves the Poisson equation to obtain the electrostatic potential. The results obtained for argon as working gas showed that for temperatures above ~1350 K in the plasma, the atomic ion is predominant [1]. The molecular ion plays a role the cold region near the tube wall. Since most of the plasma flow in the source is hot, the present studies were performed in the framework of a one-ion plasma chemistry. Solutions were obtained in the 2D planar and in the 3D geometry shown in Fig. 2. The model was realized on the computational platform COMSOL Multiphysics® [2].

3. Experiment

The gas temperature in the part of the tube outside the waveguide and in the plume region was determined by optical emission spectroscopy. An optical emission spectrometer (a 500 mm imaging spectrograph SP-2556 by Roper Acton is combined with an intensified CCD camera PI-MAX4:1024i-RB by Princeton Instruments) is used to record the plasma emission. The light from different positions either inside the quartz tube or in the plasma plume is focused by a quartz lens (l= 50 mm) placed behind a 10 mm iris at a distance of about 250 mm from the plasma zone, on an UV-VIS fibre, which is coupled to the spectrograph. The highest possible spectral resolution (~0.03 nm, 2400 g/mm grating) of the spectrometer is used to record molecular band structures.

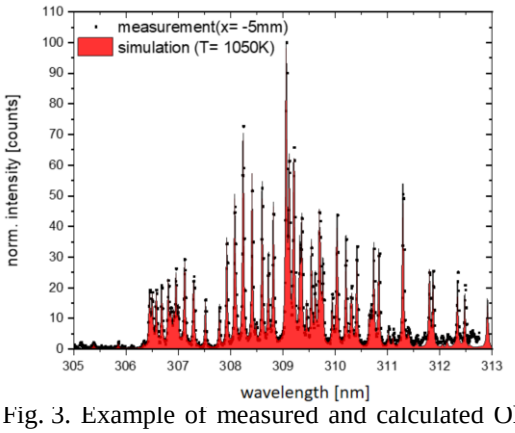

Fig. 3. Example of measured and calculated OH-spectra in the argon jet without substrate (grating 2400 g/mm, 1 kW, 18 slm Ar, L_{out}= 15 mm).

For the evaluation of the gas temperature, the rotational temperature of the OH(A-X) band with maximum intensity near 309 nm is identified by comparing recorded and calculated spectra [3]. The calculations were performed using the simulation software Lifbase [4]. The best match of an experimental spectrum with a calculated spectrum delivers the rotational temperature. A small amount of OH, which is present from water e.g. due to diffusion from the surrounding air into the plasma plume zone, allowed to determine the gas temperature in most cases. For O_2 containing gas mixtures, an overlapping of the OH(A-X) bands with Schumann-Runge bands of O_2 occurred, mainly for positions near to the plasma source. Thus, the OH band structures are accessible only downstream in the plume, while temperature determinations from spectroscopy were not possible at the tube end and at the place of the precursor feed. Fig. 3 shows exemplarily a comparison of a measured and a calculated OH spectrum for a distance of -5 mm from the tube end in pure argon.

Surface temperatures are determined by means of a thermographic camera VarioCAM by InfraTec with an effective resolution of 640x480 pixels. The measurement was set up in the temperature range from 720 to 1770 K with a rotating big quartz tube serving as deposition target.

The target is typically placed at a varying distance from the waveguide. The distance to the measurement spot is 920 mm. Time-averaged values are obtained for three positions: (1) the spot of deposition, (2) the end of the plasma torch quartz tube and (3) at the position of the local temperature maximum inside the substrate as illustrated in Fig. 4. The high sensitivity of the measurement allowed to detect even small variations of few mm in the distance of operation.

4. Results

Fig. 5 shows the gas temperature distribution obtained from the 2D planar model for pure argon with an inflow rate of 18 slm, an incoming microwave power of 1 kW and the length L_{out}=38 mm. The outflow occurs into a substrate-free space. The temperature reaches a maximum value of ~1500 K close to the inner tube wall on the side of the incoming microwaves and decreases outside the tube to temperatures far below 1000 K. The asymmetric temperature distribution in the plasma source is evident in the plume, where a shift of the hot gas flow out of the tube axis can be seen.

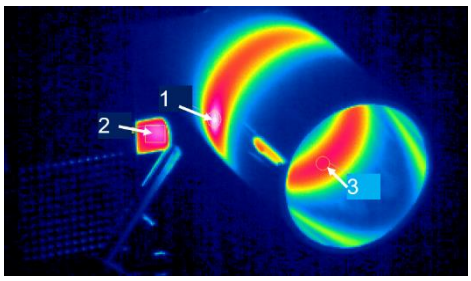

Fig. 4. Thermography at the place of deposition.

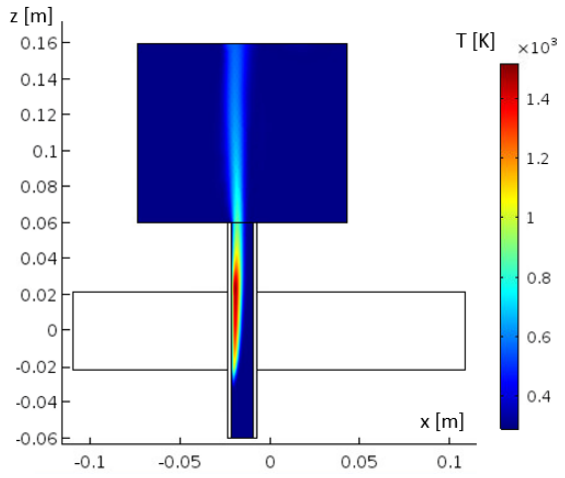

Fig. 5. Two-dimensional distribution of the gas temperature in the plasma source and in the plume for an incident power of 1 kW and a flow rate of 18 slm.

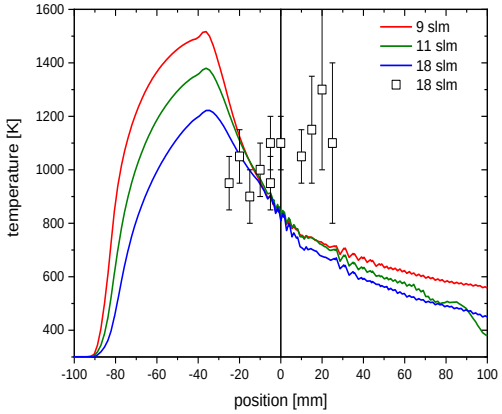

Fig. 5. Gas temperature along a line-out 2.5 mm away from the tube wall (lines) and experimental results (symbols) The position of the tube end is zero. (1 kW, L_{out}= 38 mm).

Fig. 6 presents the modelling results along a line-out 2.5 mm away from the tube wall for three different gas flow rates. For the highest flow of 18 slm Ar, the calculated gas temperatures are also compared with the temperatures obtained experimentally by optical emission spectroscopy (OES). The position of the measurements is given with respect to the discharge tube end. Interestingly, the temperature decrease between the end of the waveguide (-25 mm) and the end of the quartz tube (0 mm) predicted by the modelling cannot be found in the measured spectra. On the contrary, the gas temperatures deduced from OES shows an increase from about 1000 K inside the tube to 1200 K at the position 20 mm outside the tube. While the model predicts temperatures of about 600 K in the plume, the OES measurements yield values between 1000 and 1400 K. This quite different behaviour can be explained by the presence of the substrate during the experiments. These measured values are of the order of magnitude needed for deposition applications. An increase of the microwave power and a reduction of the flow rate lead to higher temperatures values in the plasma source and the plume. The increase of the temperature in the plasma source, however, is related to a higher heat load on the tube wall.

Further modelling studies have been performed in 3D geometry to analyse the temperature behaviour. Besides a check of the influence of the rotational symmetry in the tube, which is neglected in the 2D model, the 3D modelling approach aims to answer the question, if a swirling inflow of the gas can reduce the heat load on the tube wall. Model calculations were performed for an incoming microwave power of 1 kW with an axial inflow only as well as with an additional swirl component of the inflow velocity at the same flow rate. The results are displayed in Fig. 7. They show almost no change in the volume distribution of the gas temperature independent of the magnitude and the direction of the swirl velocity component at the inlet position. As the arrow velocity plot shows, the swirl component becomes weak in the plasma region inside the waveguide so that the outflow is preliminary axial. Moreover, a region of recirculation appears in the region close to the entrance of the gas flow into the waveguide to the side of the shorted end of the waveguide (cf. Fig. 2). The recirculation occurs probably due to the expansion of the plasma region with the gas heating.

Therefore, the window of operation is restricted by the flow rate. Low flow rates enable higher gas temperatures, but can lead to critical heat loads on the wall of the quartz tube. This was verified by OES measurements. A decrease of the gas flow by about 20 % resulted in an increase of the gas temperature by 100 K.

Further experimental studies have shown that a decrease of the diameter of the quartz tube from 12.2 to 10 mm leads to an increase of the gas temperature by about 400 K. This finding can be seen from Fig. 8.

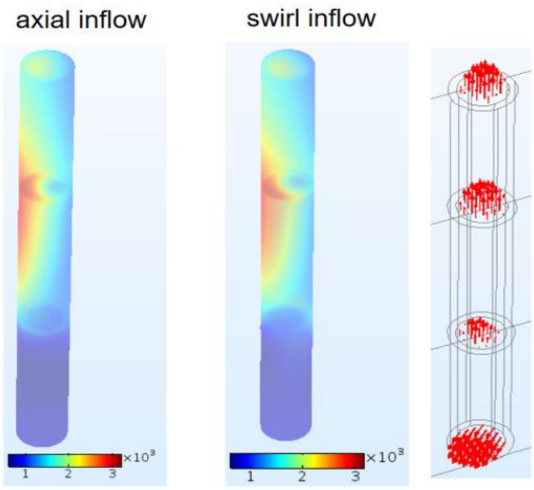

Fig. 6. Temperature [K] in the plasma source from 3D modelling with axial and swirling inflow.

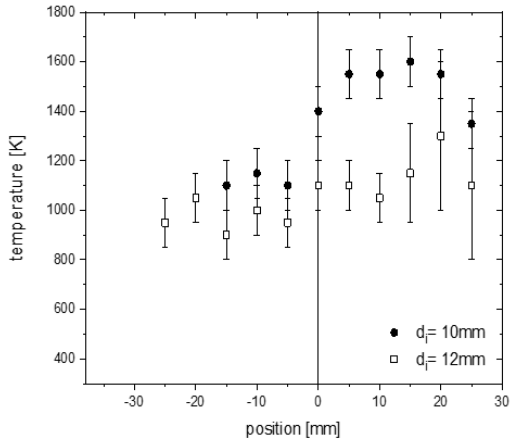

Fig. 8. Gas temperature for different tube diameters along the gas flow. The position of the tube end is zero. (1 kW, 18 slm Ar, L_{out}=38 mm).

The admixture of oxygen to argon causes a significant change of the plasma and its properties. Fig. 9 shows the results of the gas temperature determination by OES in pure argon (open squares) and in Ar/O_2 mixtures with varying oxygen content of 25, 50, and 75 %. As mentioned above, the gas temperature could only be determined from OH emission far away from the tube end, where the emission from molecular oxygen (Schumann-Runge system) is absent. The gas temperature in the source gas mixture is found to be substantially higher for every admixture of oxygen than for pure argon. This result can probably be explained by the heat released in the reactive plasma due to dissociation of oxygen molecules. The temperature values for the different admixtures of oxygen are similar within the accuracy of the measurement. The temperature decrease from ~3500 K (x= 25 mm) to 2400 K (x= 65 mm) is nearly linear with the distance. No plasma emission can be observed at a distance of x= 70 mm or higher.

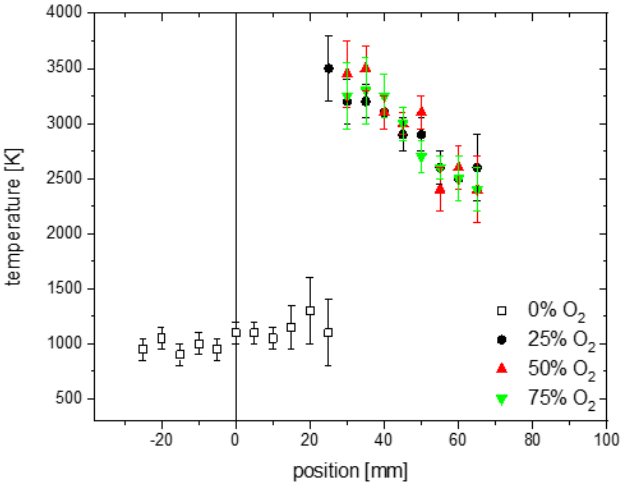

Fig. 7. Gas temperature in Ar/O_2 mixtures along the gas flow. The position of the tube end is zero. (1 kW, 18 slm, L_{out}= 38 mm).

Fig. 10 shows the surface temperature of the quartz substrate obtained by thermographic measurements for various distances between the end of the discharge tube and the substrate. It should be noted that contrary to the results shown in Fig. 9, the oxygen flow through the plasma source was kept constant and the argon was added via the precursor tube (cf. Fig. 1) in order to simulate the effects that might occur with precursors for silica. Two well-pronounced effects are observed. On the one hand, the surface temperature is largest in pure oxygen and decreases with the increase of the Ar concentration. On the other hand, the surface temperature decreases if the distance to the substrate is increased due to a reduced heating by the plasma jet.

Fig. 10. Surface temperature of the substrate for mixtures

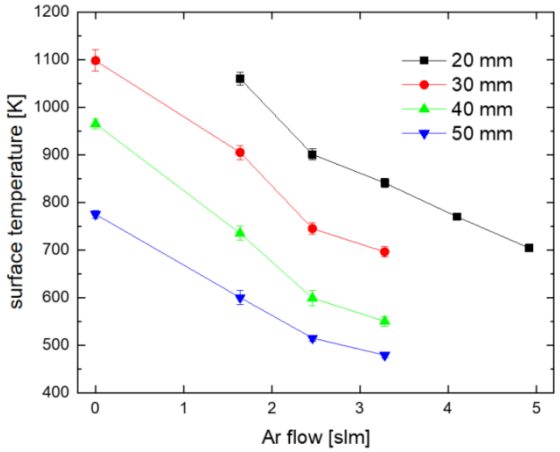

of 10 slm O_2 and varying flow of Ar fed through the precursor tube and different distances between the end of the quartz tube and the substrate (1 kW power).

5. Outlook

Since gas temperatures were not determined in oxygen-containing mixtures with the admixture of any precursor materials so far, future observation will be expanded to such application-oriented plasmas. Additionally the influence of a deposition target on the plasma and its temperatures will be investigated in more detail.

6. Acknowledgment

This work was supported by the Leibniz-Gemeinschaft: SAW-2017-IPHT-1.

7. References

[1] M Baeva, F Hempel, H Baierl, T Trautvetter, R Foest, D Loffhagen, J Phys D: Appl Phys, **51**, 385202 (2018).

[2] COMSOL Multiphysics v. 5.3a. (Stockholm: COMSOL). http://www.comsol.com.

[3] S Pellerin, J M Cormier, F Richard, K Musiol, J Chapelle, J Phys D: Appl Phys, 29, 726 (1996).

[4] LIFBASE (version 1.9), J Luque, D R Crosley, SRI International Report MP 99-009 (1999) http://www.sri.com/cem/lifbase.